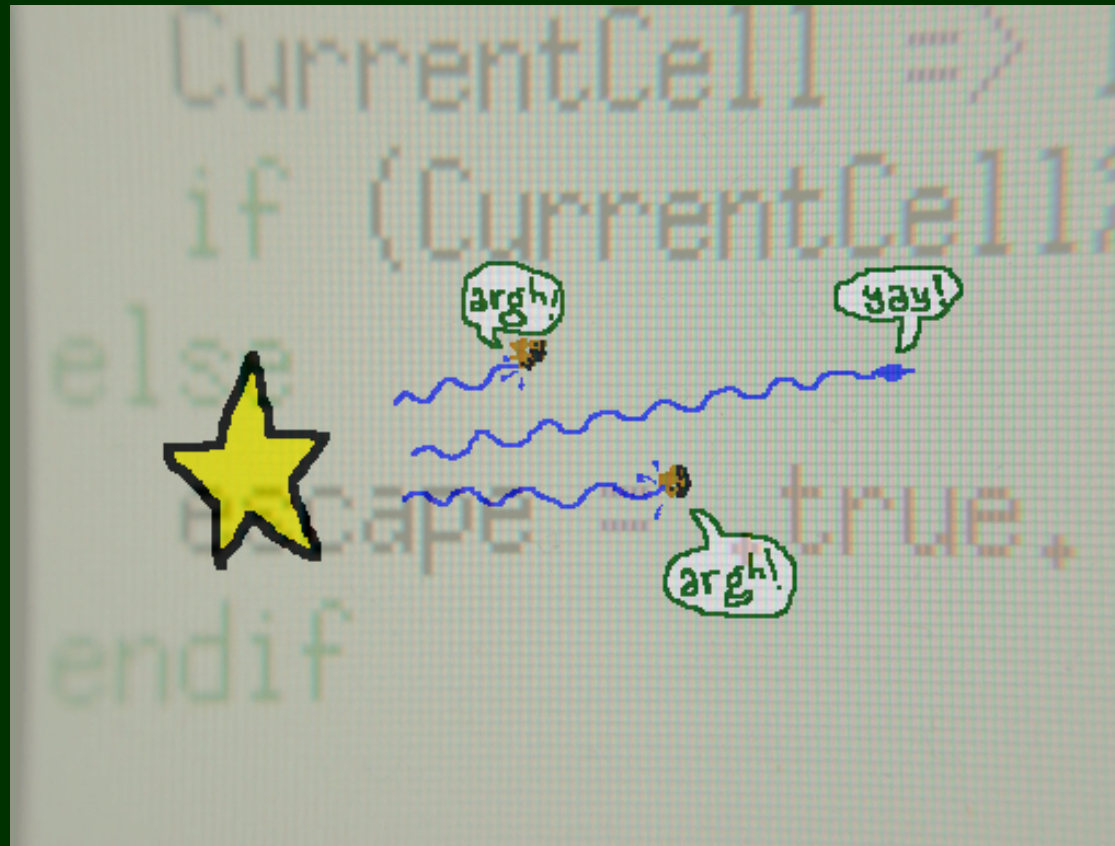


Lyman α — The Great Escape



Dark Cosmology Centre

Peter Laursen – Paris, 2009

Ly α escape from high- z galaxies

Why?



What?

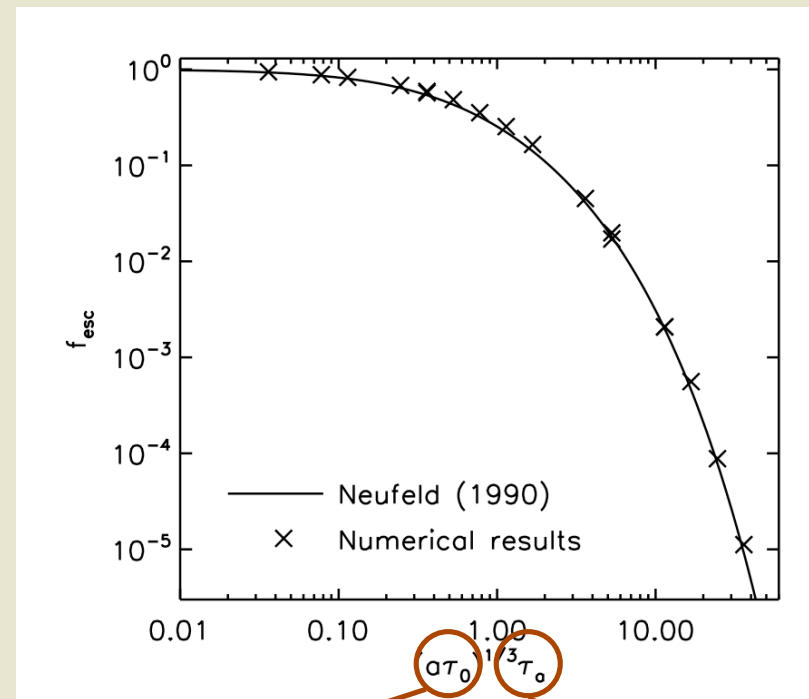
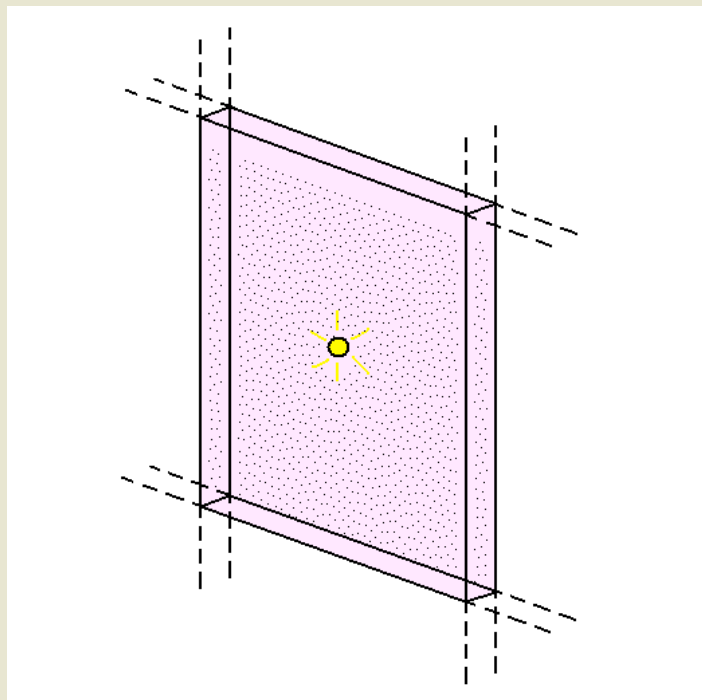
$$f_{\text{esc}} = \frac{n_{\text{ph,esc}}}{n_{\text{ph,em}}}$$

How?



Ly α escape from high- z galaxies

Analytical attempt (Neufeld 1990)



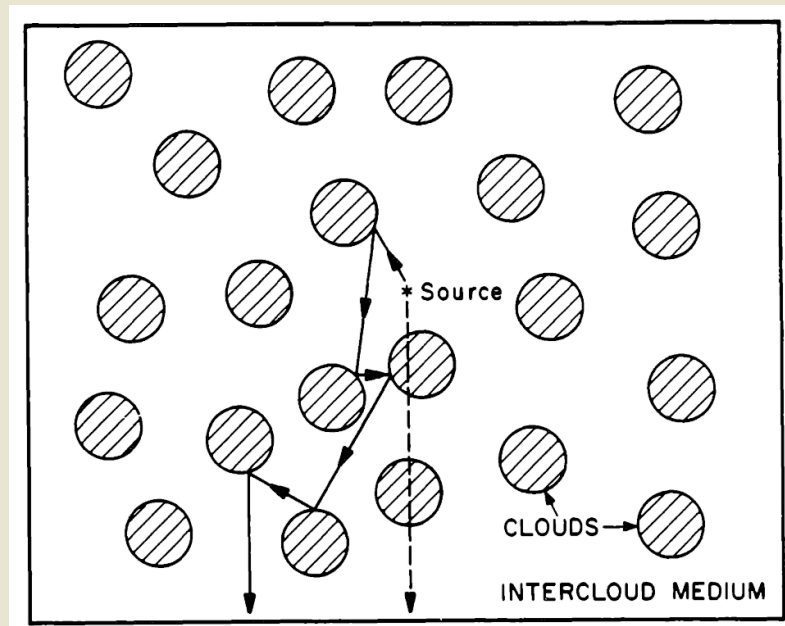
Gas density and temperature

Dust density and cross-section

Ly α escape from high- z galaxies

– Why does Ly α escape after all?

Multiphase medium?

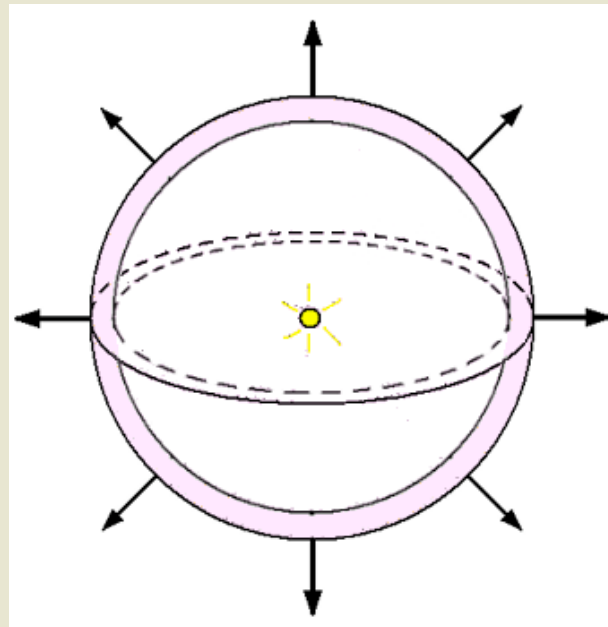


Neufeld (1991);
Hansen & Oh (2006)

Ly α escape from high- z galaxies

– Why does Ly α escape after all?

Outflow?

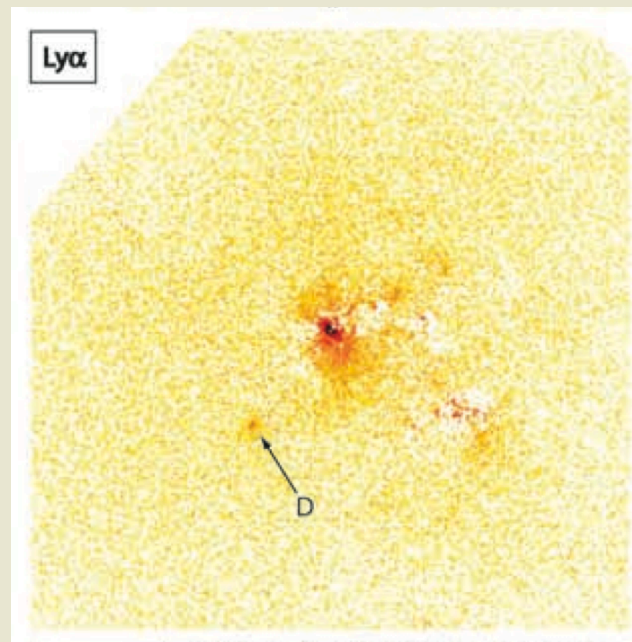


Kunth et al. (1999);
Verhamme et al. (2006);
Östlin et al. (2008)

Ly α escape from high- z galaxies

– Why does Ly α escape after all?

Ionized holes?

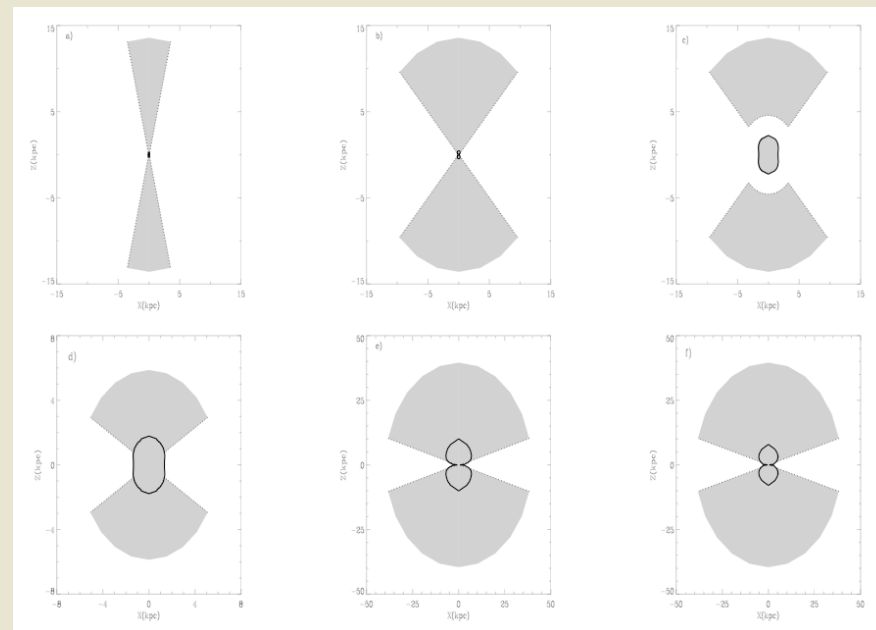


Kunth et al. (2003);
Hayes et al. (2007)

Ly α escape from high- z galaxies

– Why does Ly α escape after all?

Ionized cones +
viewing angle?

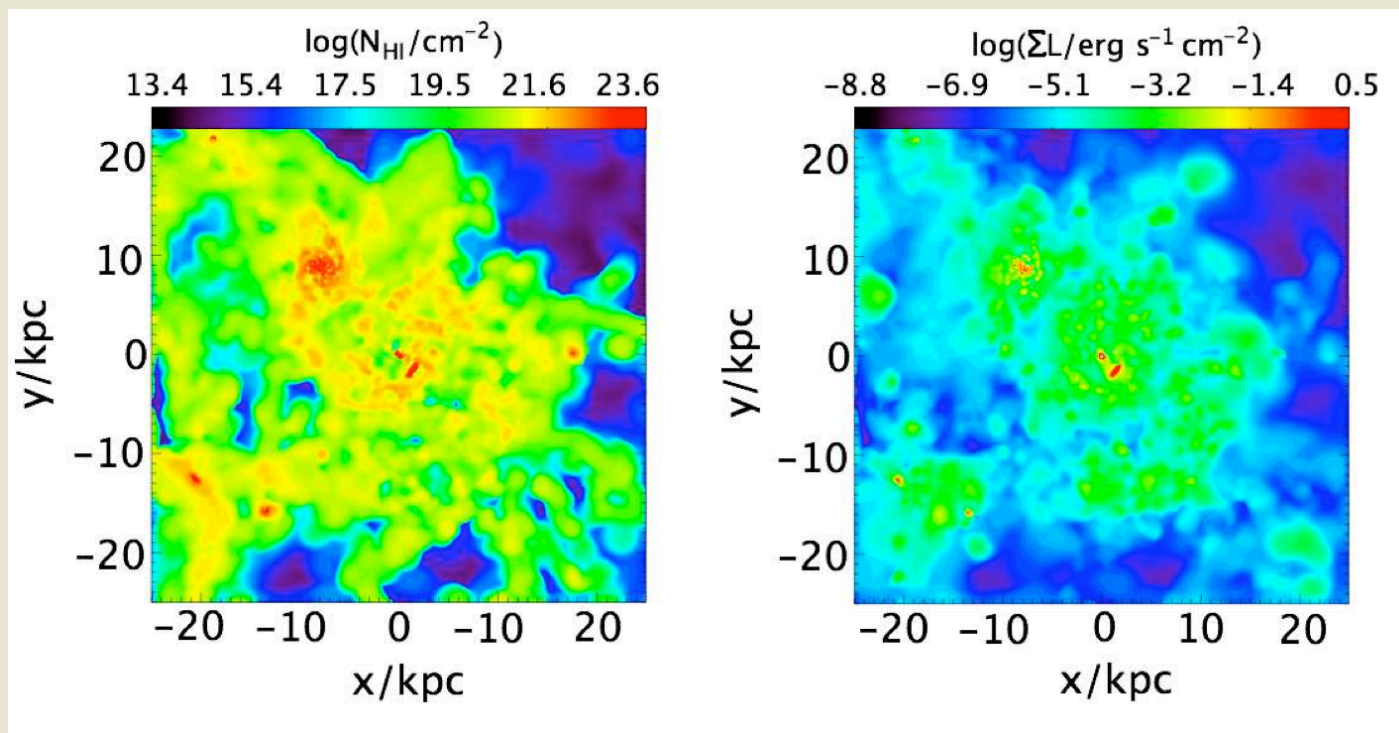


Tenori-Tagle et al. (1999);

Mas-Hesse et al. (2003)

Numerical approach

Cosmological **N-body** + **hydro** simulation
+ Ly α **RT** on **AMR** grid with **dust**



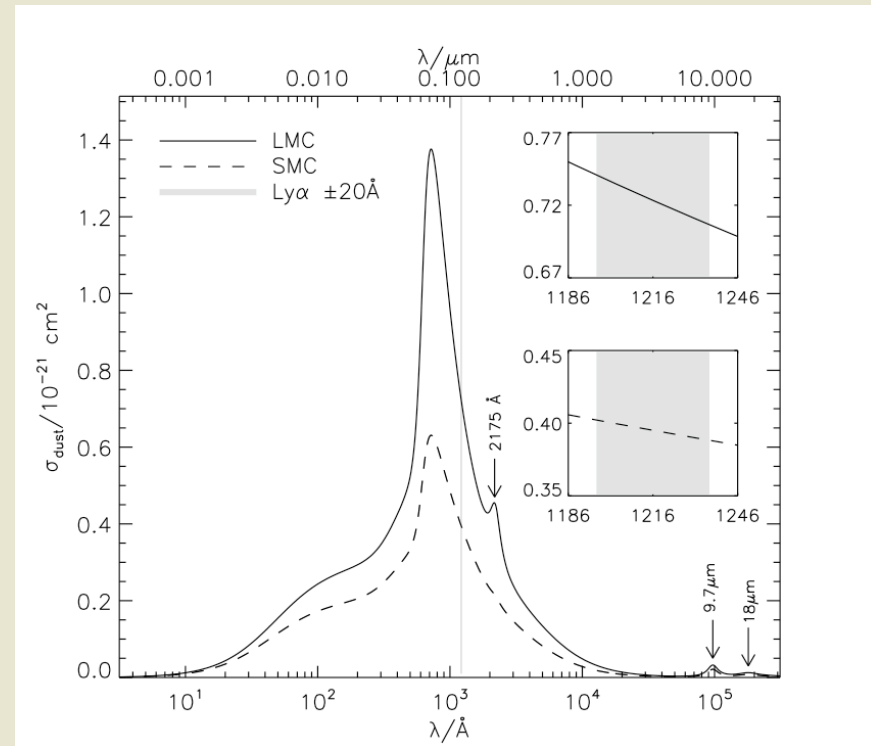
Dust

Four important quantities:

- Cross-section: $\sigma_d(\lambda)$
- Density: n_d
- Albedo: A
- Phase function: $P(\theta, \phi)$

$$A_V \propto N_H$$

e.g. Bohlin, Savage & Drake (1978)



Pei (1991) + Weingartner & Draine (2001) + Gnedin et al. (2008)

Dust

Four important quantities:

- Cross-section: $\sigma_d(\lambda)$
- Density: n_d
- Albedo: A
- Phase function: $P(\theta, \phi)$

$$n_d \sim n_H \frac{\sum_i Z_i}{\sum_i Z_{i,0}},$$

Dust

Four important quantities:

- Cross-section: $\sigma_d(\lambda)$
- Density: n_d
- Albedo: A
- Phase function: $P(\theta, \phi)$

$$n_d = (n_{\text{HI}} + f_{\text{ion}} n_{\text{HII}}) \frac{\sum_i Z_i}{\sum_i Z_{i,0}}$$

Dust

Four important quantities:

- Cross-section: $\sigma_d(\lambda)$
- Density: n_d
- Albedo: A
- Phase function: $P(\theta, \phi)$

2.2.1. Dust in ionized gas

Ionized gas is found in a number of physically distinct locations throughout the Universe. Compact HII regions, or Strömgren spheres, surround young, hot stars, while more diffuse HII is a part of the ISM. Larger HII “bubbles” are formed around regions of massive star formation due not only to ionizing radiation from the stars but also to the energy deposited in the ISM from supernova feedback. Outside the galaxies, the IGM is predominantly ionized at $z \lesssim 5-6$. Observations show or indicate the presence of dust in all of these media. While generally lower than in the neutral gas, inferred dust-to-gas mass ratios (f_{dg}) in ionized gas span a range from roughly equal to the typically assumed MW ISM value of ~ 0.01 , to upper limits of $\sim 10^{-4}$ times lower than this.

Based on 45–180 μm (FIR) spectroscopy, Aannestad & Emery (2001) found the Galactic HII region S125 to be strongly depleted of dust, with a dust-to-gas ratio of $f_{dg} \leq 10^{-6}$, while Smith et al. (1999), using MIR imaging and spectroscopy, inferred a dust-to-gas ratio of the Galactic HII region RCW 38 of 10^{-5} to 10^{-4} . On the other hand, using FIR spectroscopy Chini, Krügel, & Kreysa (1986) found 12 HII regions to be dust-depleted by “only” a factor of 10 relative to the MW ISM (i.e. $f_{dg} \sim 10^{-3}$), while from FIR photometry, Harper & Low (1971) found the median dust-to-ionized-gas ratio of seven HII regions to be close to 0.01.

For the more diffuse HII gas that comprises part of the ISM, most obtained extinction curves in a sense already include the contribution of HII to n_d , although its quantity is not revealed when measuring HII column densities. Hence, any value of f_{ion} for the diffuse ISM larger than 0 would account twice for the ionized gas.

The dominant destruction mechanism of dust is probably shock waves, associated with, e.g., high-velocity clouds and SN winds (Draine & Salpeter 1979a,b). However, since SNe are thought to be the prime creator of dust at high redshifts, the HII bubbles in the vicinity of massive star-forming regions cannot be entirely void of dust, and observational evidence of dust related to SN remnants (SNR) and starburst regions does indeed exist. Using MIR imaging, Bouchet et al. (2006) determined the dust-to-gas ratio of SN 1987A to be $\sim 5 \times 10^{-3}$. Somewhat lower results are found in Kes 75 ($\sim 10^{-3}$ from FIR and X-ray, Morton et al. 2007) and in Kepler’s SN ($\sim 10^{-3}$ from IR and bremsstrahlung, Contini 2004). On

larger scales, the hostile environments imposed by the SNe and ionizing radiation will reduce the dust density in starburst regions. Fitting continuum SEDs, Contini & Contini (2004) found that $10^{-4} \lesssim f_{dg} \lesssim 10^{-2}$ in various starburst regions in a sample of seven luminous infrared galaxies. However, such regions are not ionized to the same level as compact HII regions and SNRs, and as argued in the case of the diffuse HII, the scaling of dust with HII to some extent already accounts for the HII.

Various feedback processes are also responsible for expelling a non-vanishing amount of metals and dust into the IGM, although inferred dust-to-gas ratios tend to be small: from IR-to-X-ray luminosities, Giard et al. (2008) inferred a dust-to-gas ratio of a few to 5 times 10^{-4} , as did Chelouche, Koester, & Bowen (2007) by comparing photometric and spectroscopic properties of quasars behind SDSS clusters. Higher (dust-to-HII ~ 0.05 in the M81 Group, Xilouris et al. 2006) — possibly expelled from the starburst galaxy M82 — and lower ($f_{dg} \sim 10^{-6}$ in the Coma cluster and even less in five other Abell clusters, Sticker et al. 2002) values are also found. Additionally, sputtering by the hot halo gas may tend to destroy primarily small grains, leading to a flattening of the extinction curve in the UV; at the Ly α wavelength, this may reduce the average cross-section by a factor of 4–5 (Aguirre et al. 2001).

For simplicity, in the RT code we will not distinguish between HII in various regions but merely settle on an average dust-to-gas ratio of ionized gas of 10^{-4} ; that is we set $f_{ion} = 0.01$. In §7, we investigate the effect of other values of f_{ion} and find that using 0.01, the resulting escape fractions lie approximately midway between those found when using $f_{ion} = 0$ and $f_{ion} = 1$. Moreover, these extreme values does not seem to change f_{esc} by more than $\sim 25\%$.

$$10^{-4} \geq f_{ion} \geq 1$$

Dust

Four important quantities:

- Cross-section: $\sigma_d(\lambda)$
- Density: n_d
- Albedo: A
- Phase function: $P(\theta, \phi)$

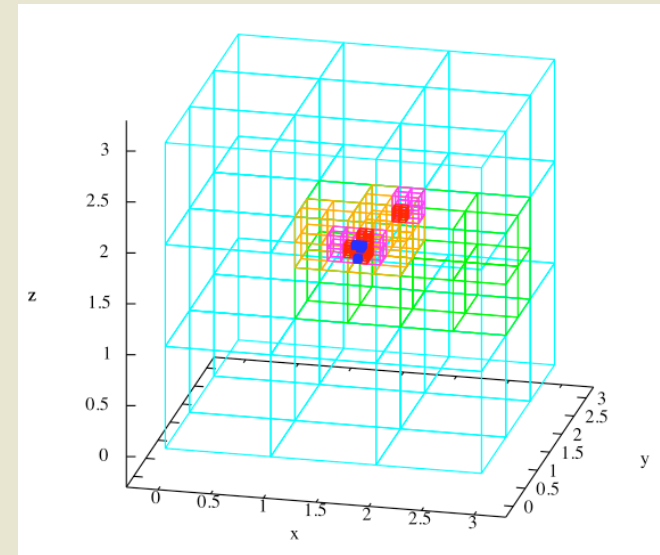
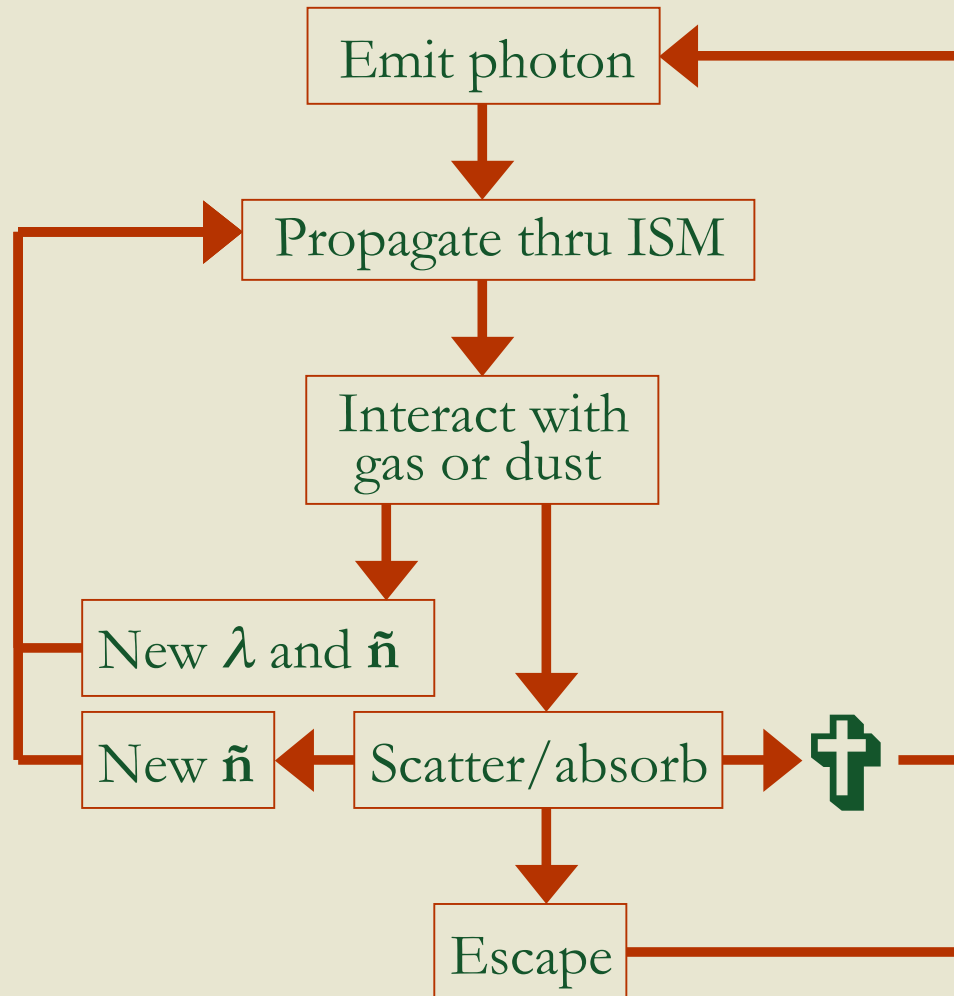


Calzetti et al. (1995); Lillie et al. (1976); Li & Draine (2001)

$$A_{\text{Ly}\alpha} = 0.32$$

$$g_{\text{Ly}\alpha} = 0.73$$

MoCALATA

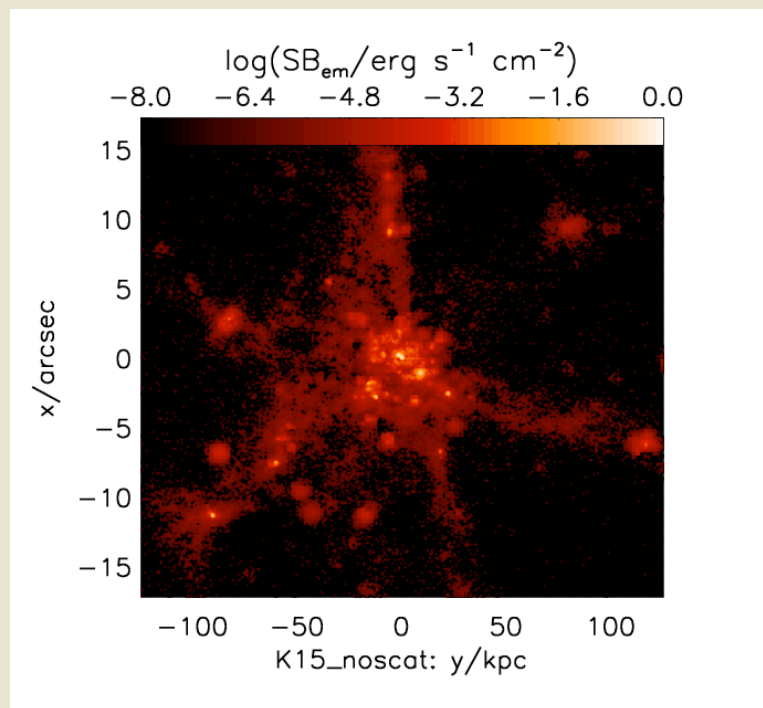


In each cell:

$$L_{\text{Ly}\alpha}, T, \mathbf{v}_{\text{bulk}}, n_{\text{HI}}, n_{\text{HII}}, Z_{\text{C,N,O,Mg,Si,S,Ca,Fe}}$$

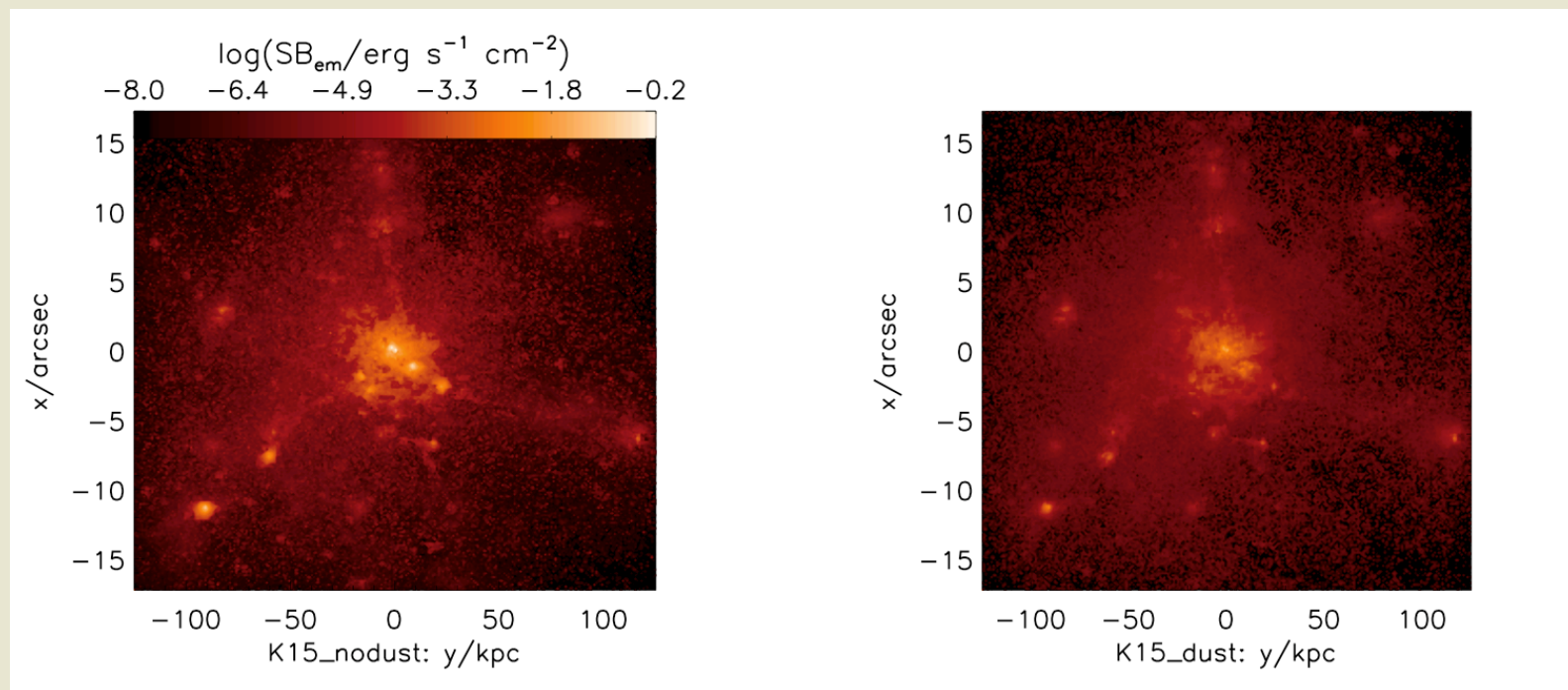
Results

Surface brightness map: *Without scattering*



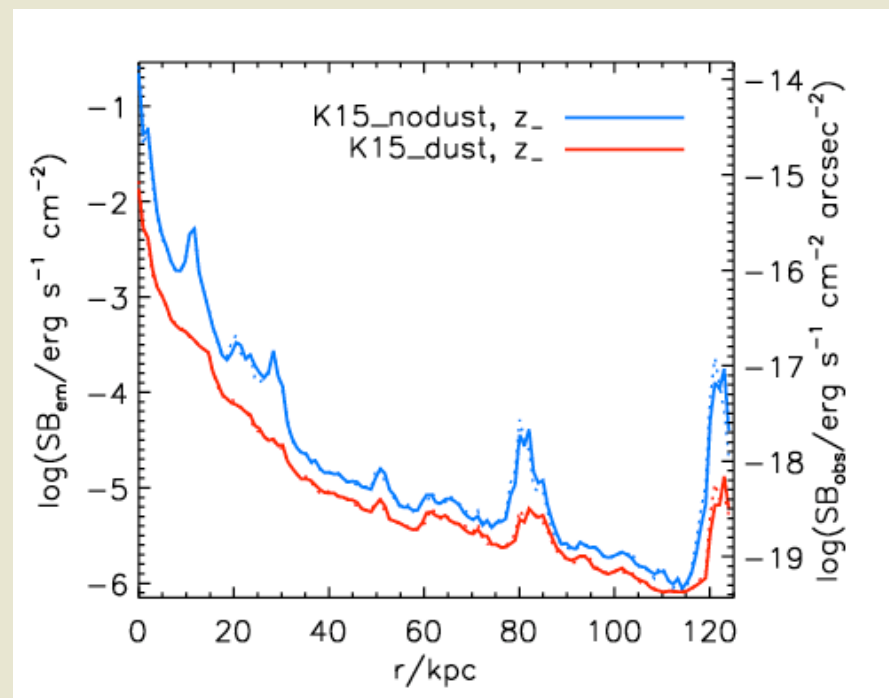
Results

Surface brightness map: *With scattering and dust; luminous regions affected more*



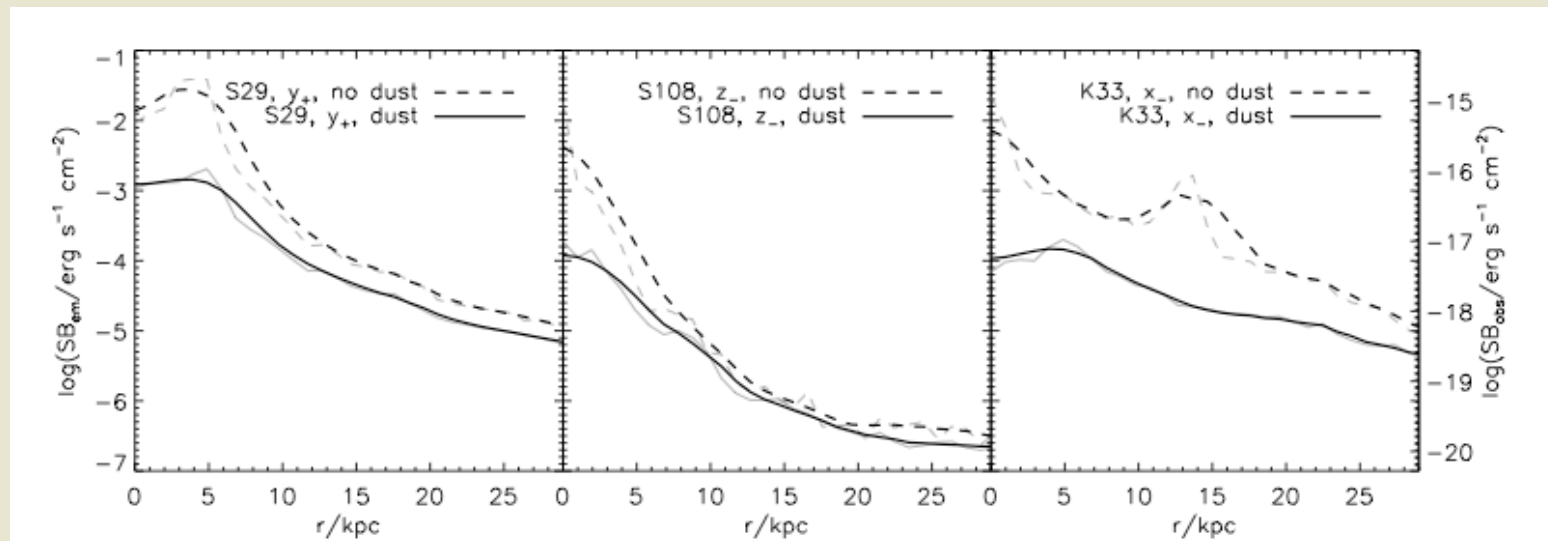
Results

⇒ Surface brightness profile: **Prominent features smoothed out**



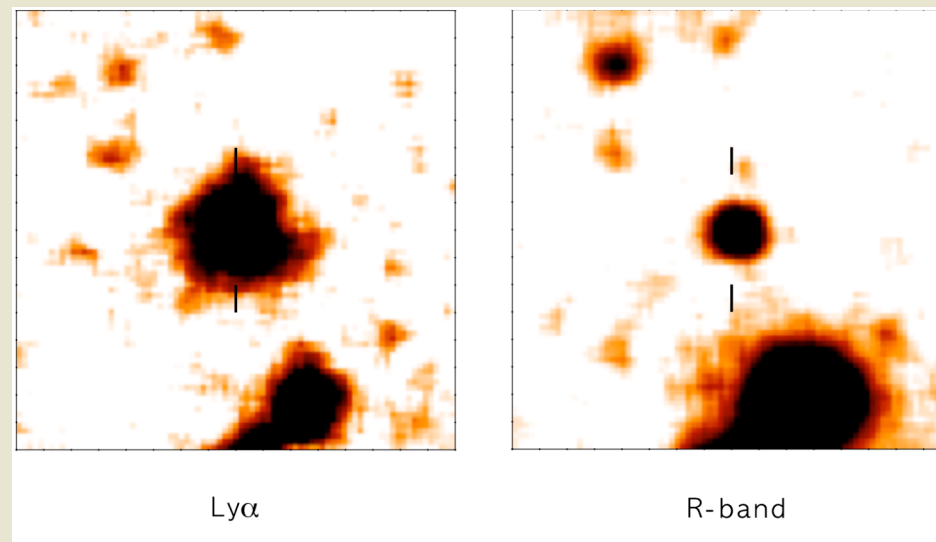
Results

Surface brightness profile: Dust helps to make profile looks more extended



Results

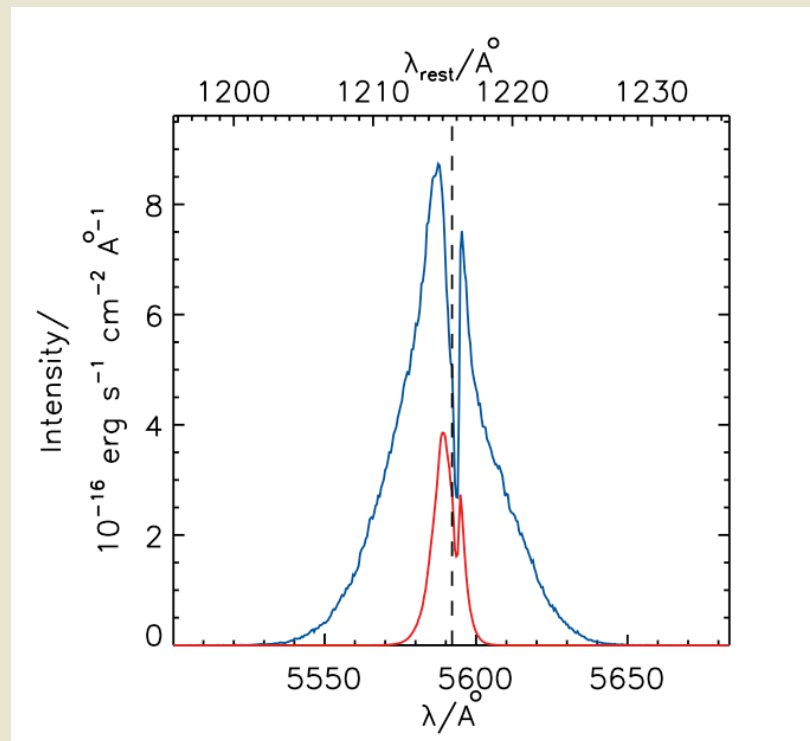
Surface brightness profile: Dust helps to make profile looks more extended



Fynbo et al. (2003)

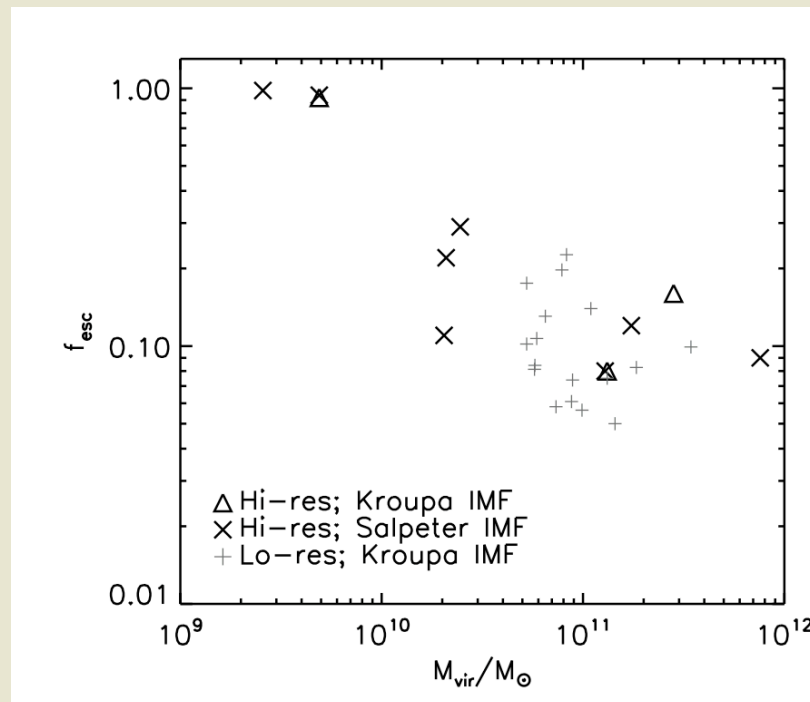
Results

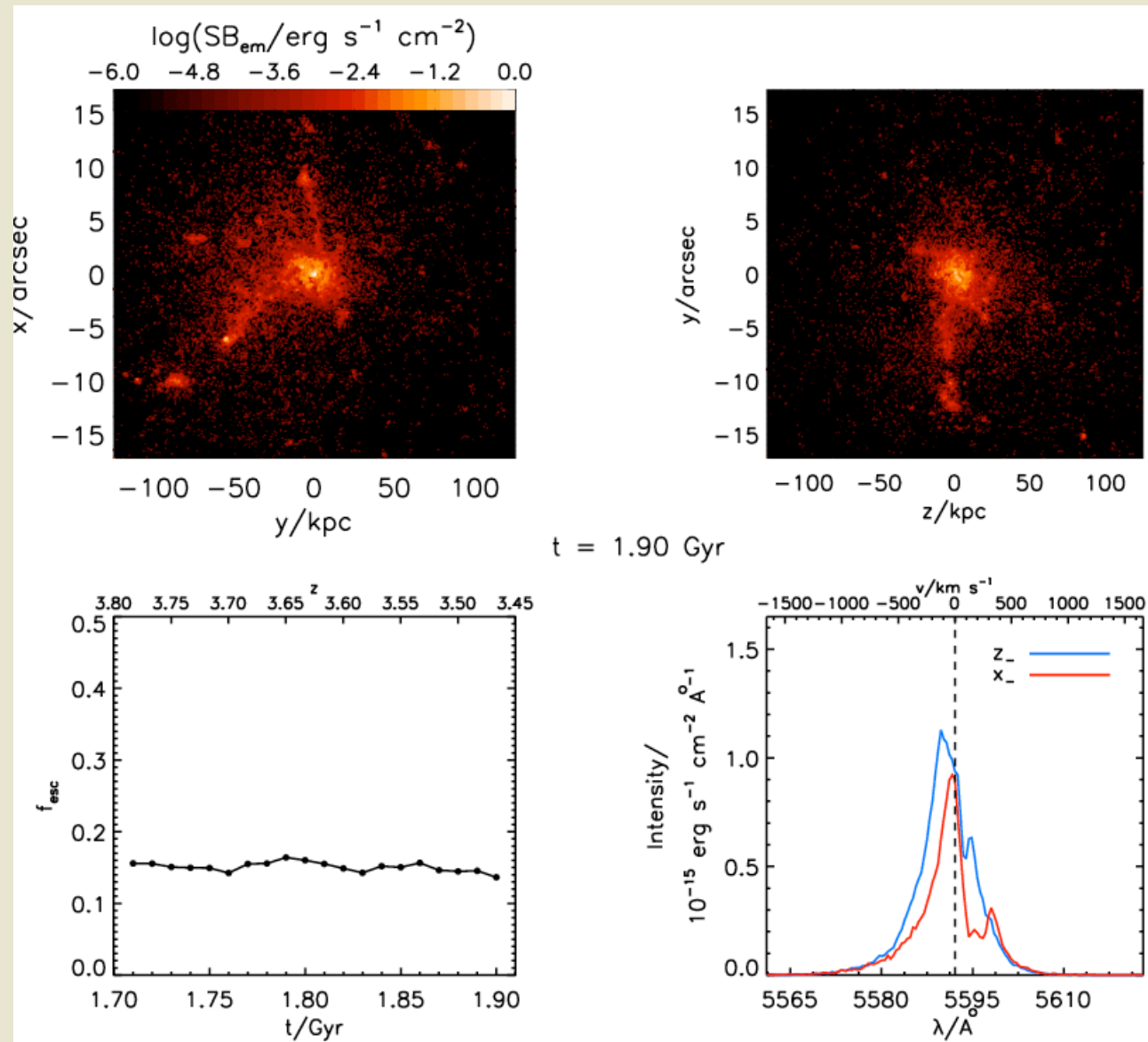
Spectrum: Escape fraction smallest in the wings



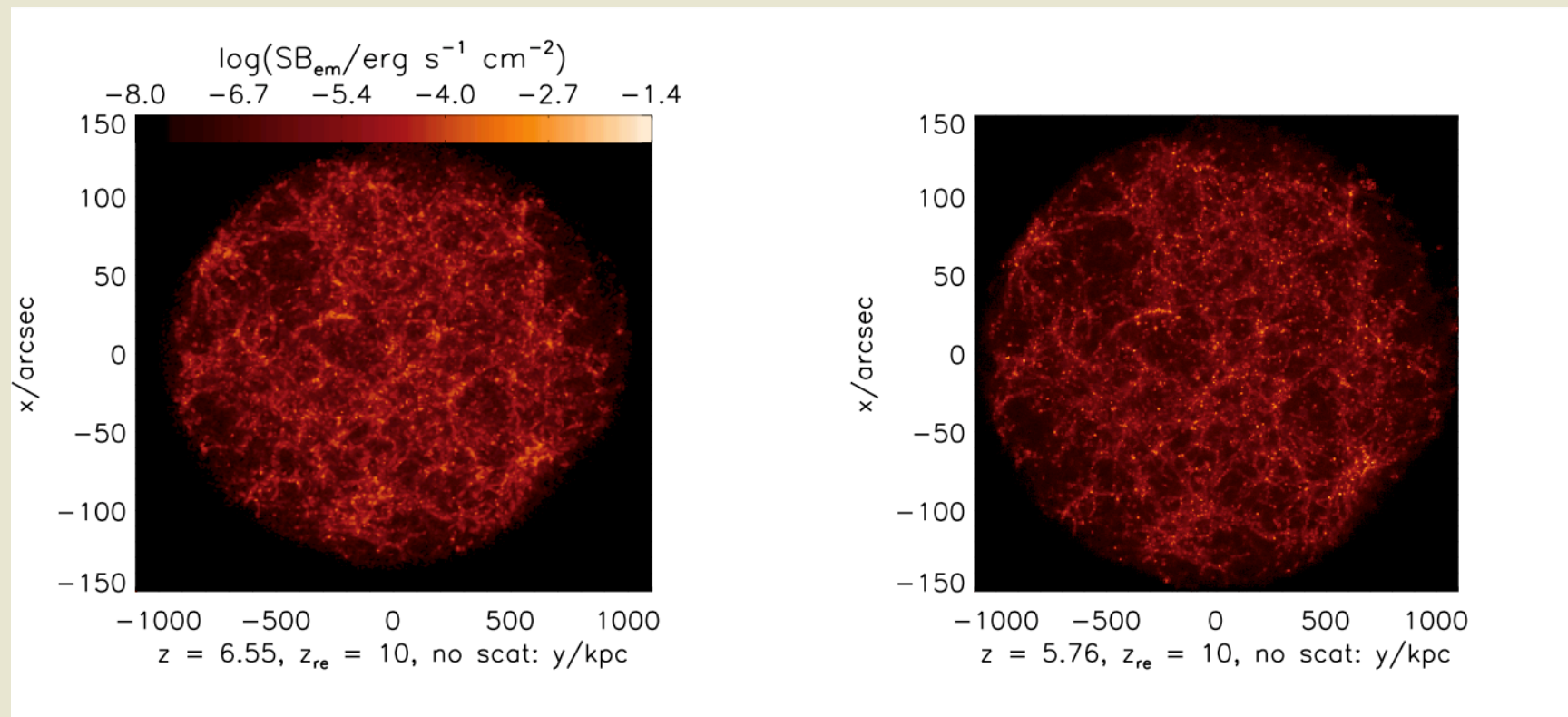
Results

$f_{\text{esc}}(M_{\text{vir}})$: Escape fraction decreases with galactic mass



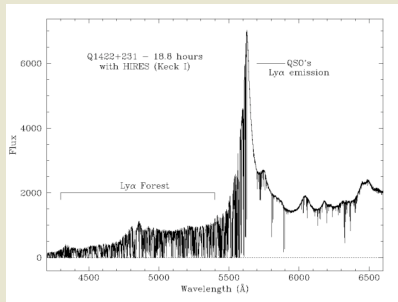


IGM transmission

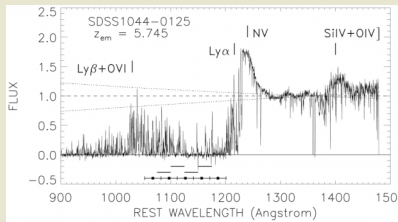


IGM transmission

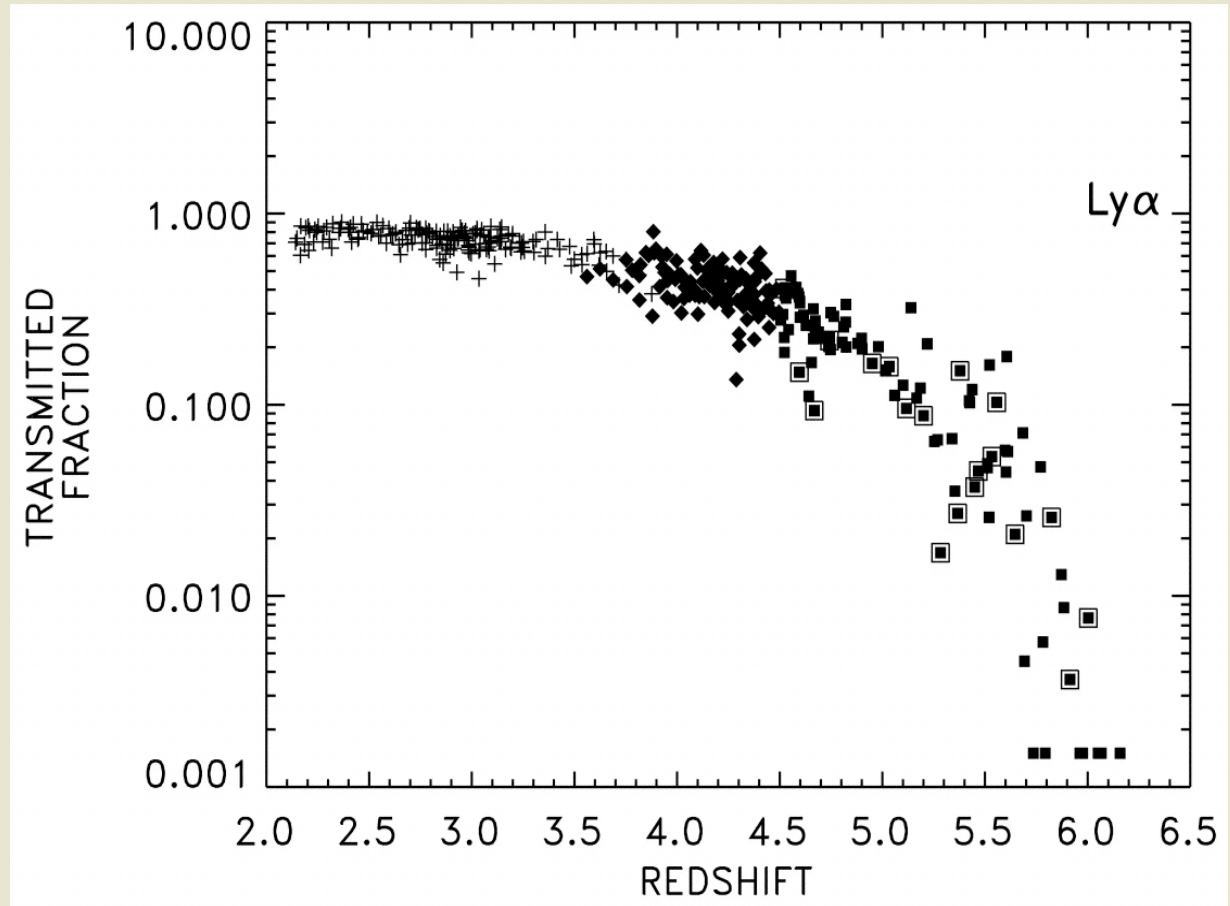
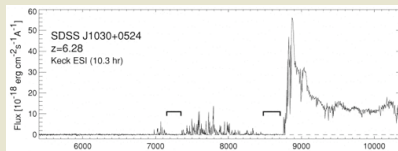
$z = 3.6$



$z = 5.7$



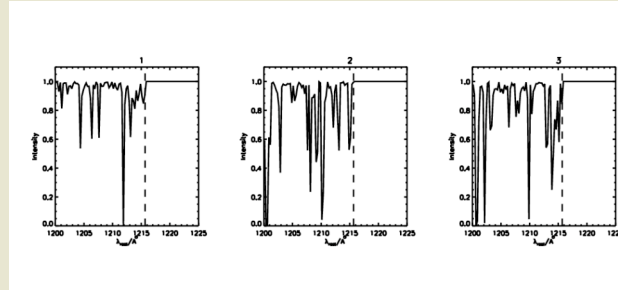
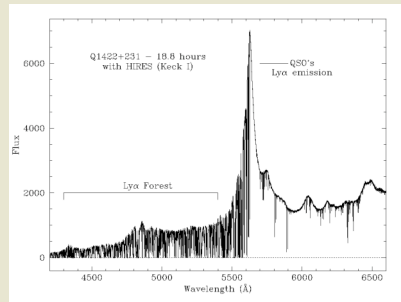
$z = 6.3$



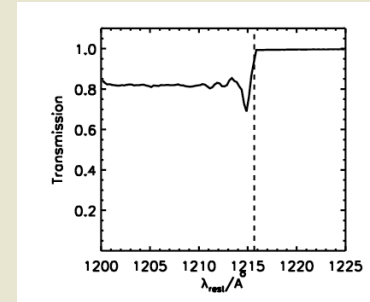
Songaila (2004)

IGM transmission

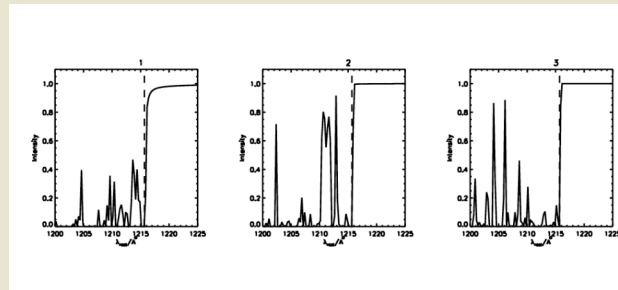
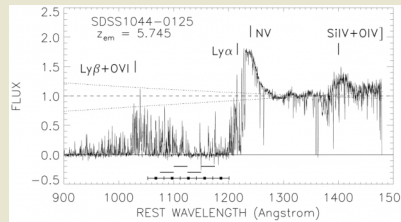
$z = 3.6$



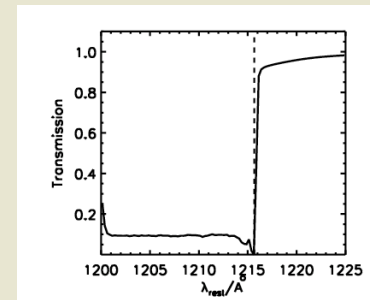
=



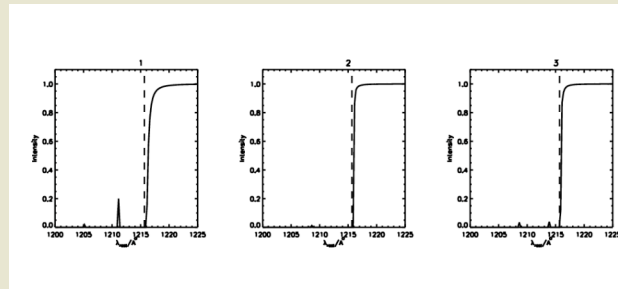
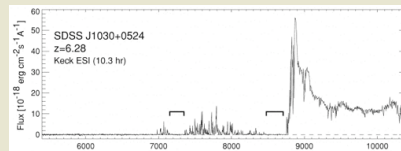
$z = 5.7$



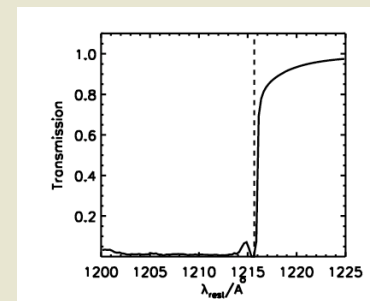
=



$z = 6.3$

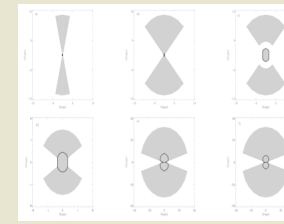
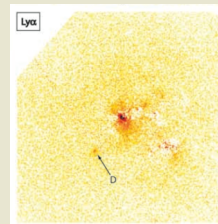
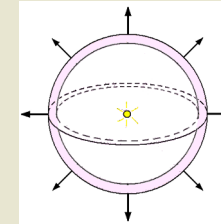
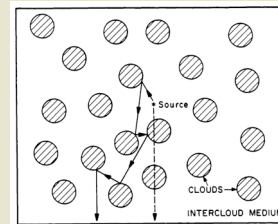


=



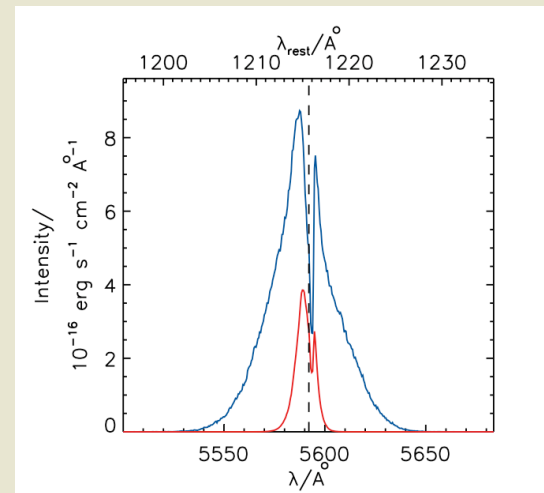
Summary

- Many factors help facilitating the escape of Ly α
 - Spectrum affected in a highly non-grey fashion
 - f_{esc} decreases with increasing M_{vir}
 - Dust makes SB profile even more extended
- Problem can be inverted: Predict results of future observations (e.g. Ultra-VISTA)
- You cannot escape the raptor



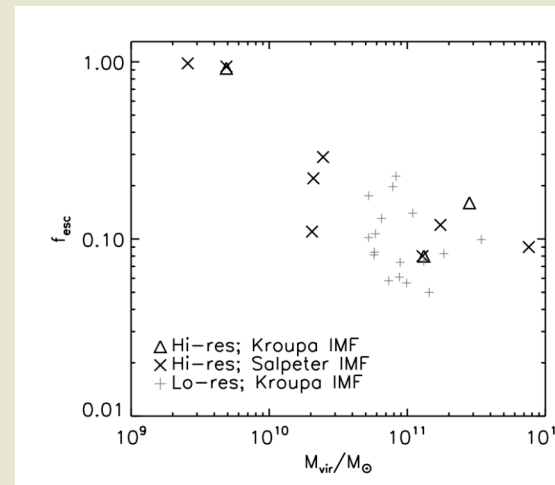
Summary

- Many factors help facilitating the escape of Ly α
- Spectrum affected in a highly non-grey fashion
- f_{esc} decreases with increasing M_{vir}
- Dust makes SB profile even more extended
- Problem can be inverted: Predict results of future observations (e.g. Ultra-VISTA)
- You cannot escape the raptor



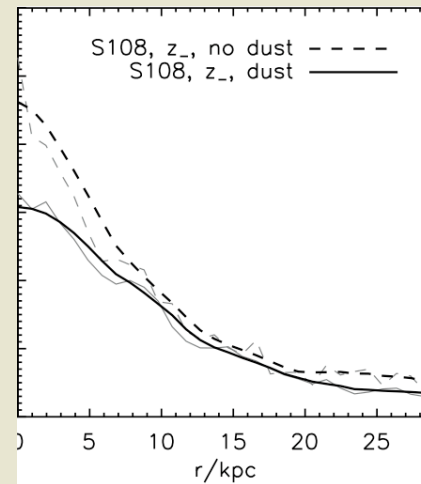
Summary

- Many factors help facilitating the escape of Ly α
- Spectrum affected in a highly non-grey fashion
- f_{esc} decreases with increasing M_{vir}
- Dust makes SB profile even more extended
- Problem can be inverted: Predict results of future observations (e.g. Ultra-VISTA)
- You cannot escape the raptor



Summary

- Many factors help facilitating the escape of Ly α
- Spectrum affected in a highly non-grey fashion
- f_{esc} decreases with increasing M_{vir}
- Dust makes SB profile even more extended
- Problem can be inverted: Predict results of future observations (e.g. Ultra-VISTA)
- You cannot escape the raptor



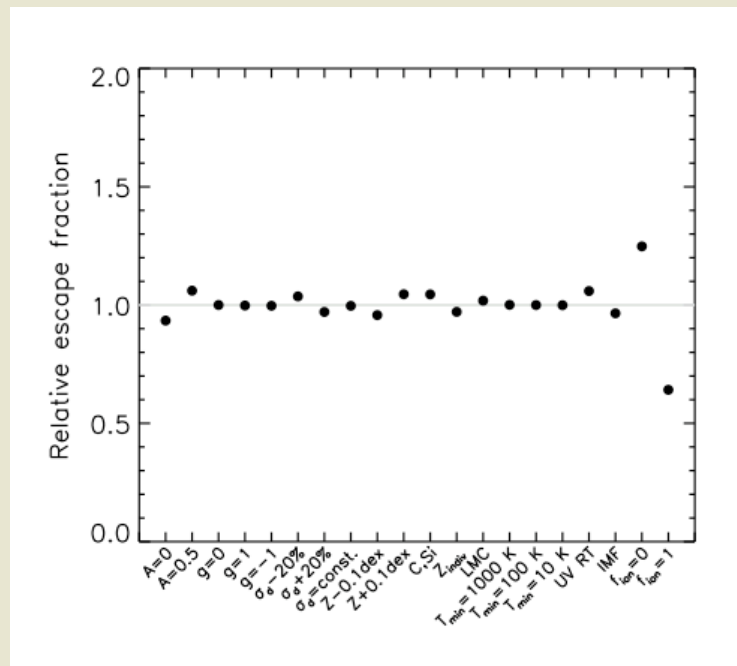
Summary

- Many factors help facilitating the escape of Ly α
- Spectrum affected in a highly non-grey fashion
- f_{esc} decreases with increasing M_{vir}
- Dust makes SB profile even more extended
- Problem can be inverted: Predict results of future observations (e.g. Ultra-VISTA)
- You cannot escape the raptor



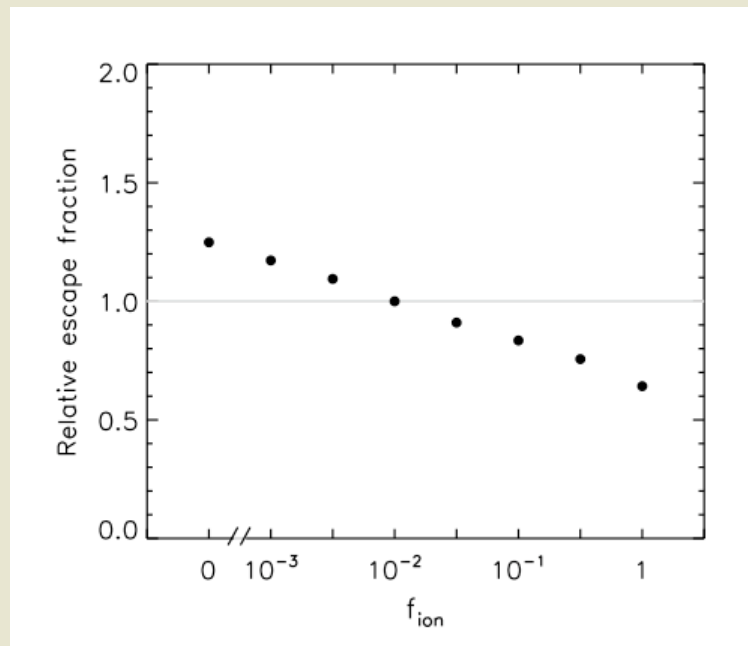
Extra stuff

Parameter study: Escape fraction quite insensitive to input parameters
(fortunately/unfortunately)



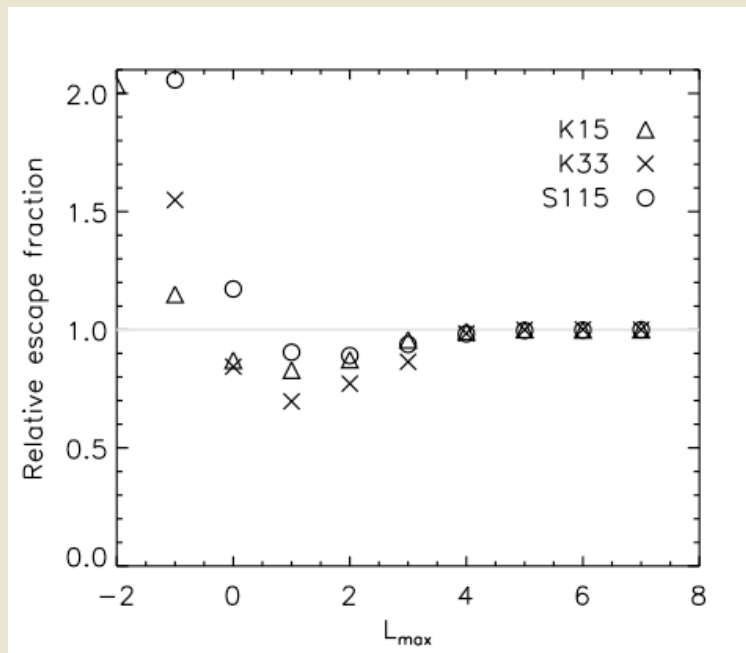
Extra stuff

Parameter study: Escape fraction quite insensitive to input parameters
(fortunately/unfortunately)



Extra stuff

Parameter study: Escape fraction quite insensitive to input parameters
(fortunately/unfortunately)



Extra stuff

Simulation parameters (in case of obnoxious question):

TABLE 1
CHARACTERISTIC QUANTITIES OF THE SIMULATIONS

Galaxy	S33sc	K15	S29	K33	S115	S87	S108	S115sc	S108sc
$N_{p,tot}$	1.2×10^6	2.2×10^6	1.1×10^6	1.2×10^6	1.3×10^6	1.4×10^6	1.3×10^6	1.3×10^6	1.3×10^6
N_{SPH}	5.5×10^5	1.0×10^6	5.1×10^5	5.5×10^5	6.4×10^5	7.0×10^5	6.3×10^5	6.4×10^5	6.3×10^5
m_{SPH}, m_{star}	5.4×10^5	9.3×10^4	9.3×10^4	9.3×10^4	1.1×10^4	1.2×10^4	1.2×10^4	2.6×10^3	1.5×10^3
m_{DM}	3.0×10^6	5.2×10^5	5.2×10^5	5.2×10^5	6.6×10^4	6.5×10^4	6.5×10^4	1.4×10^4	8.1×10^3
$\epsilon_{SPH}, \epsilon_{star}$	344	191	191	191	96	96	96	58	48
ϵ_{DM}	612	340	340	340	170	170	170	102	85
l_{min}	18	10	10	10	5	5	5	3	2.5

NOTE. — Total number of particles ($N_{p,tot}$), number of SPH particles only (N_{SPH}), masses (m), gravity softening lengths (ϵ), and minimum smoothing lengths (l_{min}) of dark matter (DM), gas (SPH), and star particles used in the simulations. Masses are measured in $h^{-1}M_{\odot}$, distances in h^{-1} pc.

TABLE 2
PHYSICAL PROPERTIES OF THE SIMULATED GALAXIES

Galaxy	S33sc	K15	S29	K33	S115	S87	S108	S115sc	S108sc
SFR/ $M_{\odot} \text{ yr}^{-1}$	70	16	13	13	0.5	0.46	1.62	3.7×10^{-3}	1.7×10^{-3}
M_{*}/M_{\odot}	3.4×10^{10}	1.3×10^{10}	6.0×10^9	6.5×10^9	2.5×10^8	1.8×10^8	4.9×10^8	2.0×10^7	5.9×10^6
M_{vir}/M_{\odot}	7.6×10^{11}	2.8×10^{11}	1.7×10^{11}	1.3×10^{11}	2.5×10^{10}	2.1×10^{10}	2.6×10^9	4.9×10^9	3.3×10^8
r_{vir}/kpc	63	45	39	35	20	19	10	12	5
[O/H]	-0.08	-0.30	-0.28	-0.40	-1.22	-1.28	-0.51	-1.54	-1.64
$V_c(z=0)/\text{km s}^{-1}$	300	245	205	180	125	132	131	50	35
$L_{Ly\alpha}/\text{erg s}^{-1}$	1.6×10^{44}	4.5×10^{43}	2.9×10^{43}	2.5×10^{43}	1.3×10^{42}	1.1×10^{42}	2.6×10^{42}	4.9×10^{40}	3.2×10^{39}
$L_{\nu,UV}/\text{erg s}^{-1} \text{ Hz}^{-1}$	5.0×10^{29}	6.7×10^{28}	9.3×10^{28}	5.5×10^{28}	3.6×10^{27}	3.3×10^{27}	1.2×10^{28}	2.6×10^{25}	1.2×10^{25}

NOTE. — Star formation rates (SFRs), stellar masses (M_{*}), virial masses (M_{vir}), virial radii (r_{vir}), metallicities ([O/H]), circular velocities (V_c), Ly α luminosities ($L_{Ly\alpha}$), and UV luminosities ($L_{\nu,UV}$) for the simulated galaxies. All quoted values correspond to a redshift of $z = 3.6$, except V_c which is given for $z = 0$.